ROLLING-BALL RUBBER-LAYER ISOLATION SYSTEM – SMALL DEFLECTION AND VIBRATIONAL BEHAVIOUR

Marco DONÀ[1], Alan H. MUHR[2], Giovanni TECCHIO[3] and Gabriele GRANELLO[4]

Abstract: The small-deflections behaviour of the Rolling-Ball Rubber-Layer (RBRL) seismic isolation system is investigated through numerical analyses, performed on the test results of a previous shaking-table experimentation, and by monoaxial sinusoidal tests specifically carried out at TARRC. The efficacy of the RBRL system in seismic mitigation is shown even for seismic events that induce only small deflections across the isolators (i.e. < 5mm). This good performance is due to the indentations developed by the balls in the rubber track under static load, caused by relaxation phenomena of the rubber. This peculiarity makes the system much more effective at low excitations than an equivalent sliding isolation system. Other useful conclusions were obtained from tests about the influence of: load on each ball, type of rubber and dwell time under static load. Finally, the results show a good retention of performance of the system when retested 15 years after its manufacture. The system, suitable for isolating light structures, is relatively economical and is easy to tailor for the specific case, in terms of geometry and performance, a great range of equivalent natural frequencies and coefficients of damping being achievable.

Introduction

The rolling-ball rubber-layer isolation (RBRL) system, originally proposed by Prof. A.G. Thomas, was developed at TARRC to enable isolation of low-mass (< 10 t) structures. The system comprises RBRL bearings and rubber recentering springs; these may be combined in single packages as shown in Figure 1 (Donà et al., 2014). The principal device components are better visible in the simplified representation of Figure 2 (Guerreiro et al., 2007); their principal functions are:

- steel rolling balls system – enables support of gravity loads and accommodation of large horizontal displacements;
- rubber-layer tracks – provide appropriate energy dissipation capacity and adequate resistance for horizontal non-seismic actions;
- rubber springs – provide recentering function and system stiffness in steady-state rolling phase.

The device assembly is relatively economical and is easy to tailor for the specific case, in terms of geometry and performance. Depending on the choice of parameters, the RBRL system provides a rich variety of possibilities, including primary seismic mitigation strategies of isolation, damping or fuse functions.

Extensive experimental studies of this system were undertaken by TARRC and collaborating research centres in the period 1995 – 2002 (Donà et al., 2014), resulting in four publications on shaking table tests and two more publications restricted to laboratory characterisation of the system itself. The systems studied were diverse, involving different design natural frequencies and levels of damping. Large amounts of data were gathered, most notably on

[1] Ph.D. Student, Dept. ICEA - University of Padova, Padova (IT), marco.dona@dicea.unipd.it
[2] Head of Engineering Design Unit, Tun Abdul Razak Research Centre (TARRC), Brickendonbury-Hertford (UK), amuhr@tarrc.co.uk
[3] Ph.D., Dept. ICEA - University of Padova, Padova (IT), giovanni.tecchio@dicea.unipd.it
[4] Master Graduate, Dept. ICEA - University of Padova, Padova (IT), gabriele.granello@dicea.unipd.it

the ECOEST project, and only a summary of the findings with a few highlights has so far appeared in the literature.

In this paper further analyses of the results of the ECOEST project are presented in order to more clearly establish the performance of the system for small seismic excitations. Secondly, new monoaxial sinusoidal tests on the same RBRL devices manufactured for the ECOEST project are presented, with the aim to better characterize the small-deflections behaviour of the system; different test velocities, loads per ball and types of rubber were considered. Some useful considerations are also given regarding the influence of the dwell time of the static load on the system behaviour. Finally, another experiment concerning the stability of the system performance, after 1000 sinusoidal loops at small amplitudes, is shown and discussed, taking into account also the possibility to use such system as an anti-vibrational device.

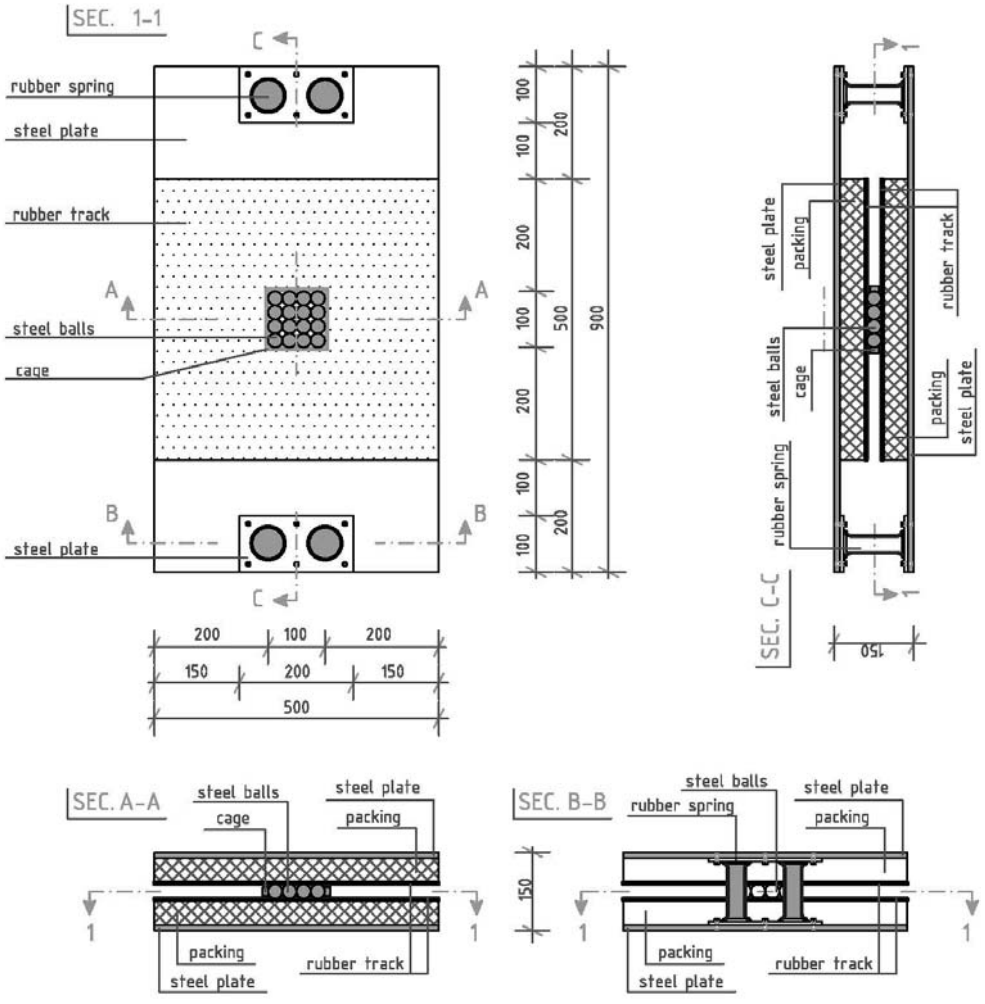

Figure 1. Combined package of RBRL bearing and recentering springs as used for REEDS and ECOEST projects, by Donà et al. (2014).

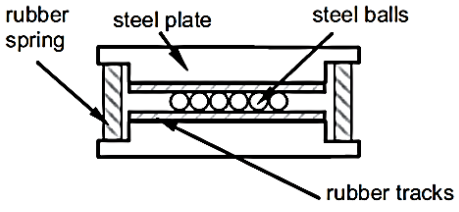

Figure 2. Simplified representation of the RBRL system (from Guerreiro et al. 2007).

Advantageous behaviour of the RBRL system for small deflections

The model superstructure in the ECOEST project (Guerreiro et al., 2007) consisted of two concrete slabs which could either be clamped together (Mass Down configuration) or separated by four M16 studs 500 mm long, as in Figure 3 a), to give a first mode fixed base response at ~2.5 Hz (Mass Up configuration). Both the configurations, isolated on the RBRL system, were subjected to a range of acceleration time histories. The results recorded (see Figure 3 a) consist of relative displacements, between the bottom slab and the shaking table and between the two slabs, and of absolute accelerations of table, bottom slab and top slab.

ECOEST data for the Mass Up configuration, for peak accelerations of the shaking table, lower and upper slab, and for the drift between the slabs, were compared to results from OpenSees simulations of the relative "fixed-base" case (Figure 3 b). The time histories were truncated in this exercise such that steady-state rolling of the balls did not occur, but they merely rocked in the "pits" formed in the rubber tracks due to creep in the rubber for the period under static load. The maximum displacement of the lower mass relative to the table for this to be so, was taken in this exercise to be 5 mm. The measured table accelerations were used in the OpenSees simulations, rather than the command time histories, to make the comparison as close as possible. The fixed-base case represents also the behaviour of a sliding isolation system, for excitations insufficient to overcome the static friction.

The earthquakes considered were: Northridge_PCKC, Tolmezzo, Faial, EC8(05) and EC8(02) (Figure 4). Artificial records were used for EC(02) and EC(05) earthquakes, according to Eurocode 8 (Soil type B, ζ = 5%): (02) and (05) signify that the original records were applied with low frequency cut-offs of 0.2 and 0.5 Hz respectively because of the maximum displacement limitation of the table (±100mm). For each case, the original record with a given peak ground accelerations (PGA_0) was scaled to different PGA levels through the parameter K[dB] = 20·log· (PGA/PGA_0) to get a certain range of seismic intensities. The results obtained considering the first three acceleration time-series are presented in Figures 5, 6 and 7, whose captions report the values of K considered for each earthquake. The low damping rubber, type A, was used for both the rolling tracks of the devices in all the tests here considered, except for the earthquake EC8(02) where the device presented one layer of rubber A and one of high damping rubber B (Guerreiro et al., 2007).

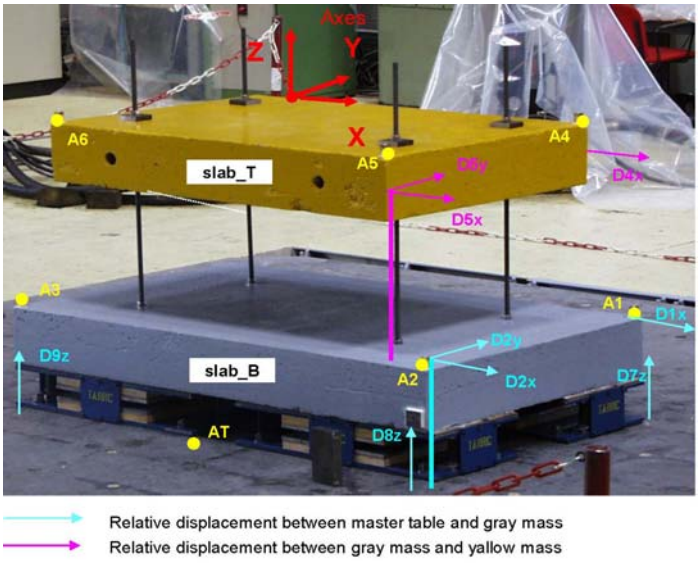

a)

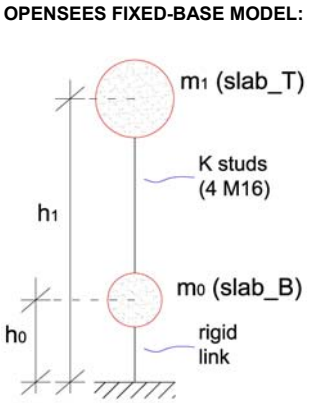

m_1 (slab_T) = 0.945 ton
m_0 (slab_B) = 0.575 ton
K (4M16) = 150 N/mm
h_1 = 100 mm
h_0 = 800 mm

b)

Figure 3. a) Mass Up configuration with transducers indication (A = accelerations; D = displacements), from ECOEST project. b) Relative fixed-base model analyzed in OpenSees for comparisons.

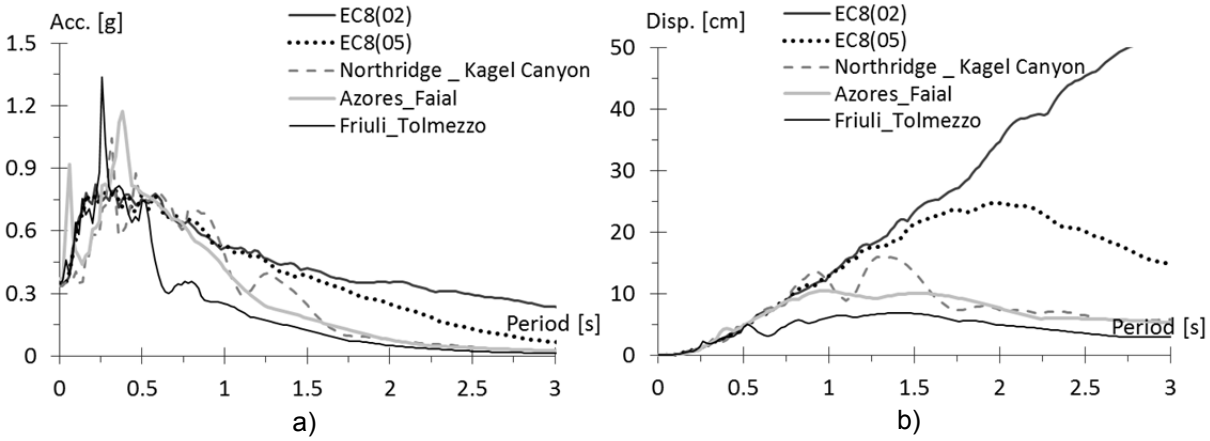

Figure 4. a) Acceleration and b) displacement response spectra of the ground motion selected for the tests with Mass Up configuration, as recorded at the table (ζ = 5%).

The parameters compared in the graphs from Figure 5 to Figure 7 are:
- for the real isolated system, by ECOEST results:
  a [g] table = accel. of the shaking table;
  a [g] slab_B = accel. of the bottom slab;
  a [g] slab_T = accel. of the top slab;
  Θ[%] Isolated= drift between the slabs as % of their separation.
- for the fixed-base system, by OpenSees simulations:
  a [g] table = accel. of the shaking table;
  a [g] slab_T_Fixed = accel. of the top slab;
  Θ[%] Fixed= drift between the slabs as % of their separation.

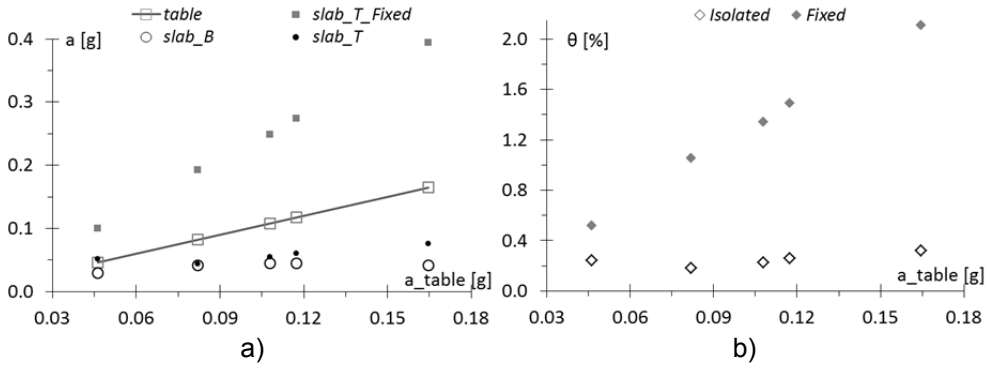

Figure 5. a) Top("T")-bottom("B") slab accelerations a[g] and b) drifts θ [%] between the two slabs versus peak table acceleration from ECOEST results, for the isolated-base case, compared with the simulated fixed-base case ("Fixed") (≈sliding isolator for small seismic intensity), for Northridge_PCKC different-scaled earthquakes (K= -12, -6, -4, -3, 0 dB).

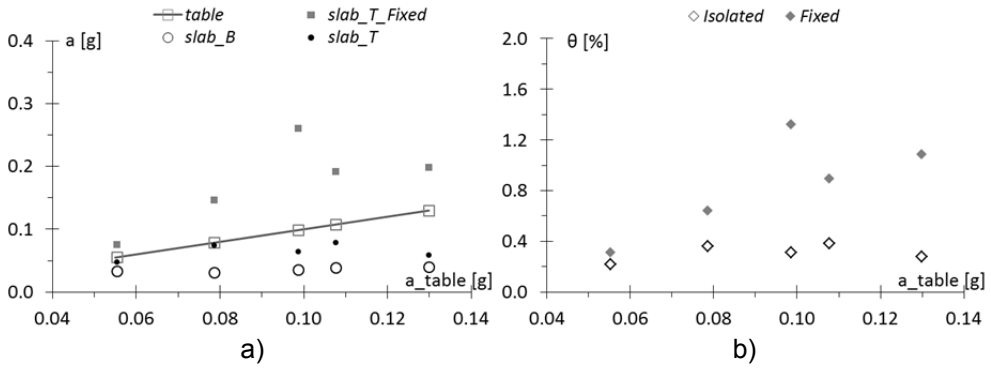

Figure 6. As Figure 5, for Tolmezzo different-scaled earthquakes (K= -12, -6, 0, +3, +5 dB).

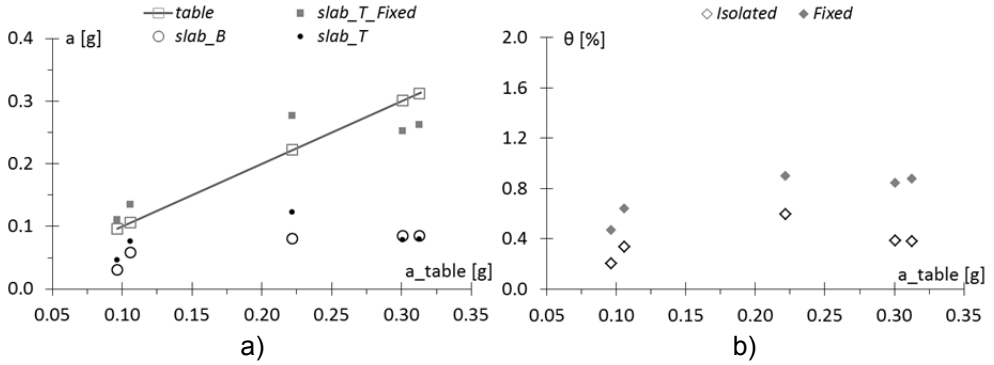

Figure 7. As Figure 5, for Faial different-scaled earthquakes (K= -12, -6, 0, +3, +3 dB).

For all the earthquakes analysed, the conclusions are the same: the compliance and damping at small excitations has the great advantage of both changing the mode shape and suppressing excitation of the vibration modes of the isolated structure even for small seismic intensities, in contrast to the case of sliding bearings below their threshold force.

Sinusoidal characterization tests at small displacement amplitudes

In the ECOEST project (Guerreiro et al., 2007) the characterisation of the RBRL system was limited to a separate test for the recentering springs done at TARRC, and to sinusoidal accelerations of the mass-down configuration on A-A rubber tracks, together with the recentering springs, carried out on the ISMES shaking table at 5 Hz. For this reason, it was decided to perform more comprehensive monoaxial sinusoidal tests at TARRC, for a Ph.D. project (Donà, 2015). Some of these tests, carried out on the same RBRL devices manufactured in 1999 for the ECOEST experimentation, are reported below.

All the tests were performed in single shear configuration for one RBRL device with no recentering springs: the test setup is shown in Figure 8. The steel roller bearings shown in figure permit translation of the tope plate in the x and z directions, but prevent rotation of it about any axis. The sinusoidal motion was controlled by the actuator and transmitted to the top steel plate of the device, that supports the weight, through a rose joint connection that permits small rotations. This connection was necessary to avoid bending stresses related to a non-perfect vertical alignment between actuator and top plate of the device, and to accommodate the small z-displacement as the balls out of and into their pits. The horizontal forces (x-axis) were measured by the multiaxial load cell placed under the bottom plate of the device, which was fixed on it. This was preferred to the direct measurement of the forces by the actuator load cell, to avoid inclusion of the friction inside the linear rolling bearings which constrain the top plate motion.

The tests are presented in Table 1: three possible combinations of the rubber layers were tested: A-A, A-B and B-B (Guerreiro et al., 2007); for each of these combinations, two different values of load per ball were used, 150 N and 250 N. In addition, three different times t_{dw} of dwelling of the load in its static configuration were tested for the cases with rubber

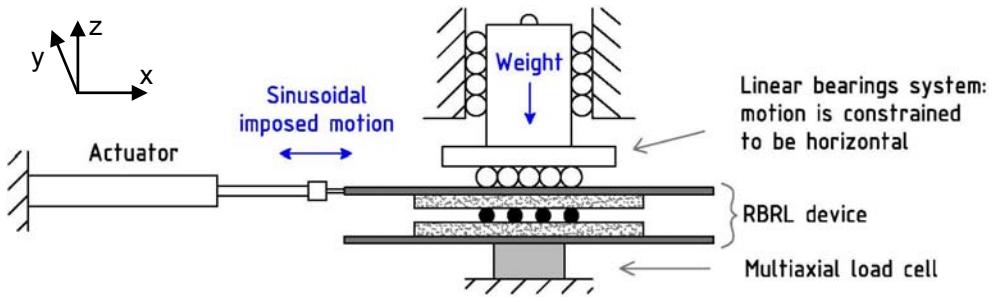

Figure 8. Schematic drawing of the setup of the sinusoidal uniaxial tests.

Table 1. Tests performed on the devices used in the ECOEST project (1999).

N° of test	Rubber Layers	Load/ball [N]	Dwell time [h]
1	A-A	150	6
2	A-A	150	24
3	A-A	150	96
4	A-A	250	6
5	A-A	250	24
6	A-A	250	96
7	A-B	150	24
8	A-B	250	24
9	B-B	150	24
10	B-B	250	24

Table 2. a) First sinusoidal input: amplitudes from 1 to 5 mm (balls rocking inside their pits).
b) Subsequent inputs: amplitudes from 6 to 70 mm.

Test Input 1			
Amplitude [mm]	Frequency [Hz]	**Max. vel.** [mm/s]	N° cycles [-]
1	5.00	**31**	3
1.5	3.33		
2.5	2.00		
5	1.00		
1	10.00	**63**	
1.5	6.67		
2.5	4.00		
5	2.00		
1	20.00	**126**	
1.5	13.33		
2.5	8.00		
5	4.00		

a)

	Max vel. [mm/s]			
	31	**63**	**126**	
	Input 2	Input 3	Input 4	
Amplitude [mm]	Frequency [Hz]	Frequency [Hz]	Frequency [Hz]	N° cycles [-]
6	0.83	1.67	3.33	3
7	0.71	1.43	2.86	
8	0.63	1.25	2.50	
9	0.56	1.11	2.22	
10	0.50	1.00	2.00	
12.5	0.40	0.80	1.60	
15	0.33	0.67	1.33	
20	0.25	0.50	1.00	
30	0.17	0.33	0.67	
40	0.13	0.25	0.50	
50	0.10	0.20	0.40	
70	0.07	0.14	0.29	

b)

tracks A-A: 6, 12 and 24 hours. The sinusoidal displacement excitations used for the tests are reported in Table 2. The first input (Table 2 a) consisted of sinusoidal cycles of very small amplitude (balls inside their pits), from 1 to 5 mm, executed at different frequencies to keep the maximum value of velocity constant: three different maximum velocities were assumed, 31.4, 62.8 and 125.6 mm/s. The other three sinusoidal inputs (Table 2 b) involved sinusoidal cycles from 6 to 70 mm and were run separately for the three maximum velocities. Each test included three sinusoidal cycles. The reason for performing the tests with amplitudes from 1 to 5 mm, for all the velocities assumed, before the other tests with constant velocity and greater amplitudes, was to study the effect of the pits on the system behaviour, it being very influenced by the rubber recovery, which will take place in a time-dependent manner as soon as the balls have rolled far enough to escape their pits.

Figures 9 and 10 show plots of the ratio $\mu = F_X/F_Z$ versus displacement x for the tests.

1) Looking at the shape of the friction-displacement (μ-disp) loops of these figures, three different situations are visible, each of them with a different shape of the associated loop; these are listed below.
- The μ-disp loops appear elliptical for amplitudes up to 5 mm or so: within this deflection the balls only rock in their pits.
- The values of μ tend to the steady-state value for displacements bigger than 15 mm: in this case the μ-disp loops consist of a first zone where the maximum force for the roll-out of the balls is developed, and a second zone characterized only by the steady-state rolling friction.

- The μ-disp loops of intermediate amplitude belong to a transition phase of the behaviour of the RBRL system. This is the most critical phase for the modelling, being highly non-linear and dependent on the viscoelastic properties of the rubber.
The peak force reached for amplitudes smaller than 5 mm appears bigger with respect to that for bigger amplitudes: this is only a consequence of the fading memory of the pit effect, once the balls have escaped the pits, and is thus due to the nature of the test input.

2) Only a very slight dependence on the velocity was seen for the steady-state rolling friction, with amplitudes bigger than 20 mm (see Figure 9). The influence of the velocity is instead not completely negligible for the determination of the peak force for the balls roll-out. This effect will be better presented and discussed in a future publication.

3) The μ-disp loops related to rubber tracks B-B (Figure 10) show much higher forces than those associated with tracks A-A, the rubber B being a high-damping compound (Guerreiro et al., 2007).

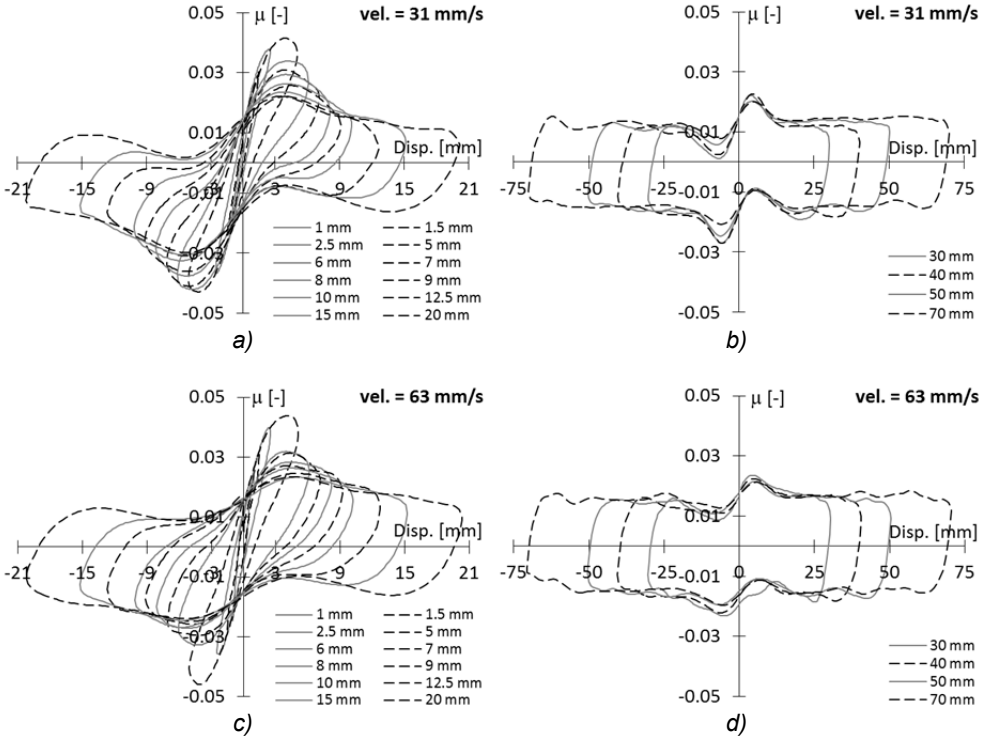

Figure 9. μ-disp loops. Case: rubber tracks A-A, W = 250 N, t_{dw} = 24 h, 2nd cycle.

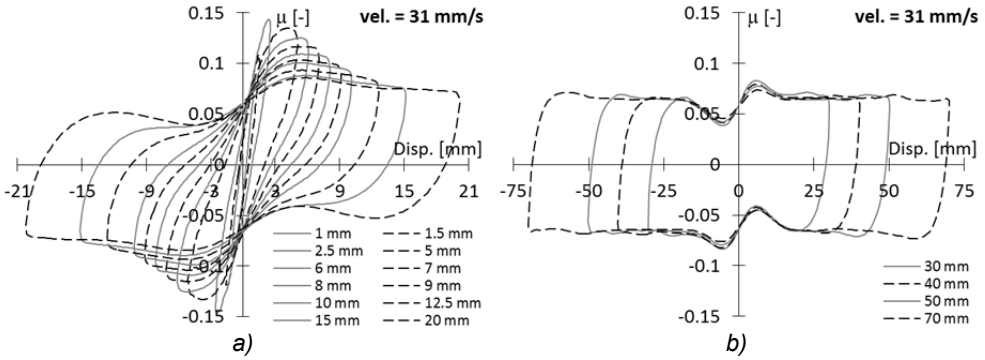

Figure 10. μ-disp loops. Case: rubber tracks B-B, W = 250 N, t_{dw} = 24 h, 2nd cycle.

ELVFD representation of the RBRL-system characteristics

To have the possibility to objectively describe and compare the behaviour of the RBRL device, shown until now through the μ-disp loops, the Equivalent Linearized Viscoelastic Frequency-Domain (ELVFD) representation was used (Donà et al. 2014, Muhr & Bergamo 2010). In particular, the Harmonic linearization method (Ahmadi & Muhr, 1997) was chosen to calculate the ELVFD parameters directly from the μ-disp loops; these parameters are: storage stiffness K', loss stiffness K'', complex stiffness K* and loss angle δ. K' and K'' are respectively defined as the in- and out-of-phase stiffness factors for calculating the "best-fit" steady-state harmonic force amplitudes required to impose a harmonic displacement of a given amplitude, i.e. the best fit elliptical approximation to the force-displacement loop. While the parameter K' is directly related to the slope (or to the stiffness) of the μ-disp loops, the stiffness K'' represents instead the energy dissipation. The magnitude of the complex stiffness |K*|, the loss angle δ and the area of the hysteresis loop A are related to K', K'' and the displacement amplitude $\tilde{x}$ by:

$$K^* = \sqrt{K'^2 + K''^2}$$
$$\tan\delta = K'' / K'$$
$$A = \pi \tilde{x}^2 K'' \qquad (1)$$

In the case of a linear viscoelastic system, K' and K'' give a perfect fit to the steady-state harmonic force, and are in general functions of test frequency. For a non-linear system, the fit is imperfect, but is often good for a fixed displacement amplitude, though K' and K'' now depend on amplitude as well as on frequency. If we consider a Kelvin model (spring and dashpot in parallel) the coefficient of critical damping ζ is approximately related to the loss angle δ by:

$$\zeta \simeq \frac{1}{2}\tan\delta \qquad (2)$$

Figure 11 gives the ELVFD representation of the RBRL system behaviour, through the parameters K', K'' and δ, for the different types of rubber track (A-A, A-B and B-B) and for both the values of the load per ball analyzed (150 and 250 N).

1) The case of the tracks B-B presents the highest values of K', K'' and thus K*, as expected. However, the loss angle δ is similar for all the rubber tracks, except for very small displacement amplitudes. As mentioned, in the case of modelling with a Kelvin model the value of δ is related to the critical damping ratio ζ; therefore, the choice of a very high-damping compound, such as type B, might not be advantageous for this scope, but could lead to some unfavourable consequences, such as excessive peak values of μ or semi-permanent deformations on the rubber layers.

2) Another useful consideration concerns the use of two different rubbers for the tracks of the RBRL device: this solution leads to intermediate results between those associated to the use of identical tracks for either type of rubber.

3) Figure 12 shows the influence of the load dwell-time on the small-deflection behaviour of the system (rubber tracks A-A and load per ball 250 N). The plots are related to amplitudes up to 5 mm, to avoid disturbance on the results because of the effects on the pits of the recovery of the rubber deformation, as explained above. While K' increases with increasing dwell time, K'' remains substantially constant; therefore, in terms of μ-disp loop for the rocking of a ball inside its pit, the dwell time seems to act only to increase the real stiffness of this loop, rather than its energy dissipation. The values of the maximum rolling friction μ_{max} are also plotted.

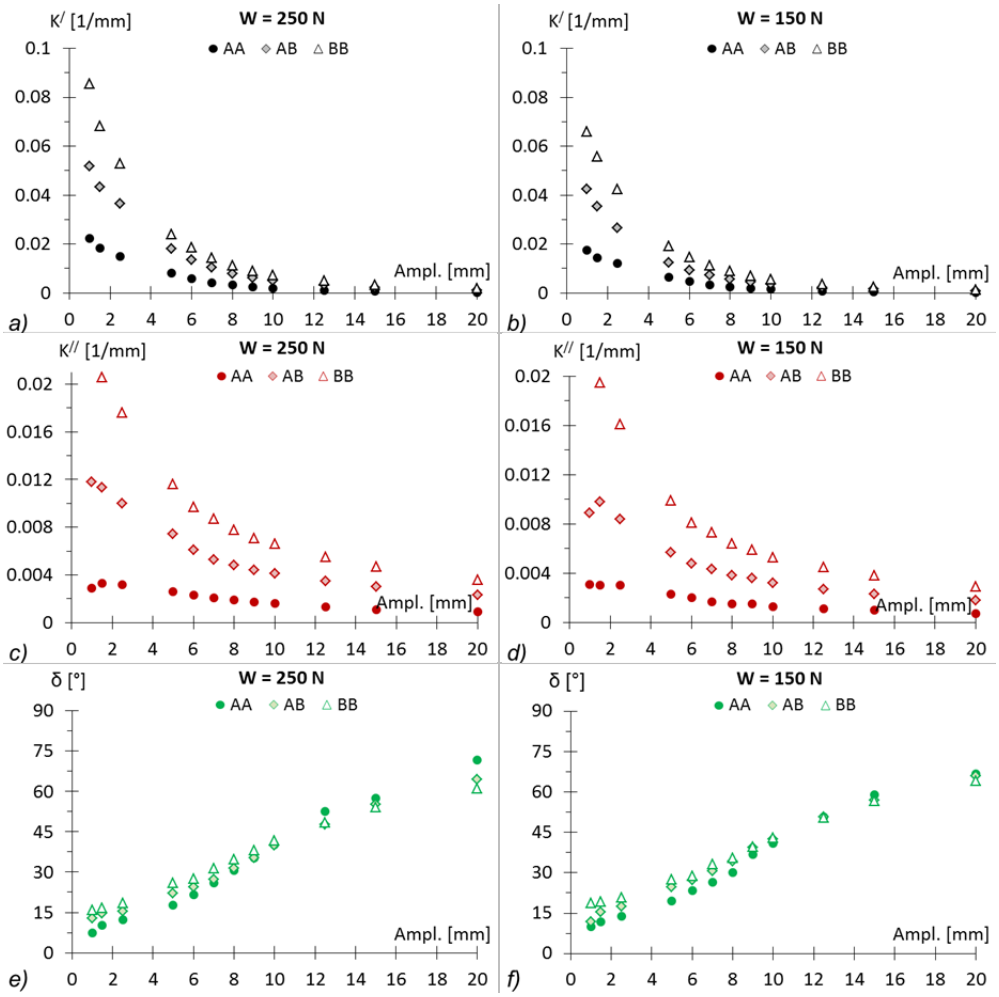

Figure 11. Comparison of $K^{/}$, $K^{//}$, δ vs amplitude, for the different rubber tracks considered: A-A, A-B and B-B. Case: t_{dw} = 24 hours, max. vel. = 31 mm/s, 2nd cycle.

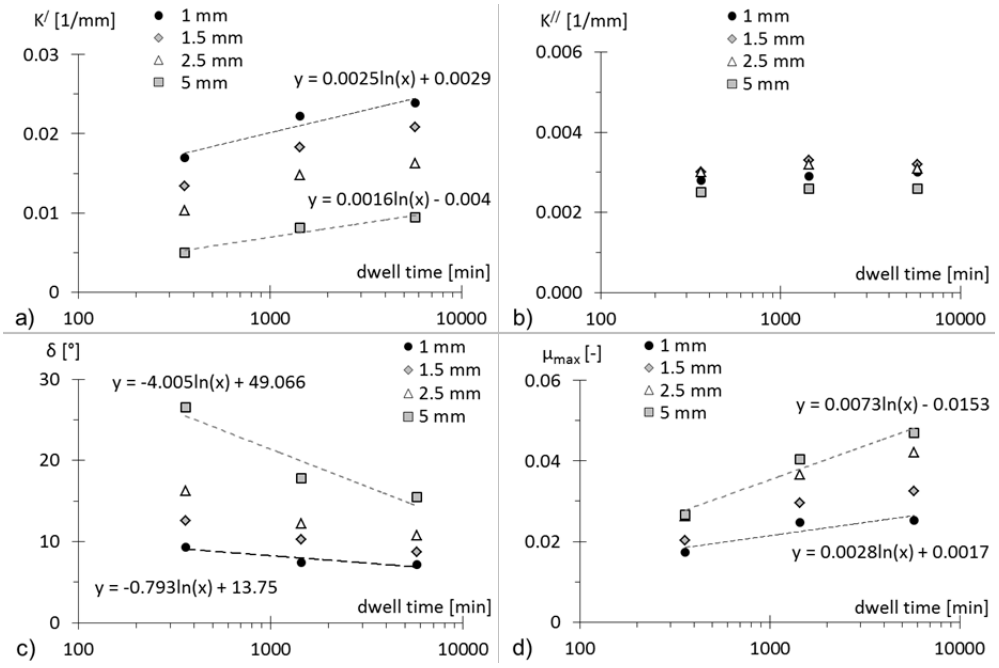

Figure 12. Dependence of $K^{/}$, $K^{//}$, δ and μ_{max} on the logarithm of the dwell time, for amplitudes up to 5 mm (balls inside pits). Case: tracks A-A, W = 250 N, max. vel.= 31 mm/s, 2nd cycle.

Stability of the system performance at small displacements

A new sinusoidal test, carried out at TARRC on a new RBRL system realized again with 2 mm thick tracks of rubber A, is briefly presented below. A stress parameter W/ER^2 (W=load per ball, E=Young modulus of rubber ≃1.12 MPa, R=radius of balls = 12.5 mm) of 1.2 was considered. The test was performed using the same setup as described above, at 2 mm amplitude and 5 Hz frequency. The results obtained, plotted in Figure 13, show a stable performance of the system still after 1000 sinusoidal vibrations at 5 Hz.

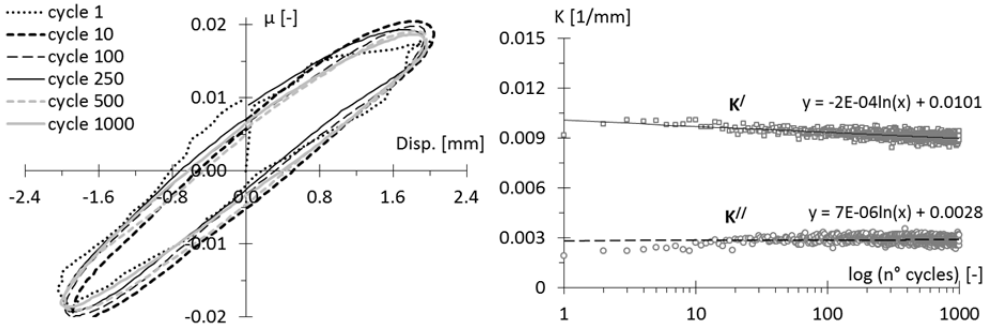

Figure 13. a) μ-disp loops and b) $K^{/}$, $K^{//}$ for a sinusoidal test at 2 mm and 5 Hz, with 1000 cycles.

Conclusions

1. The ECOEST results confirm that the RBRL isolation system provides very effective reduction of excitation of the first mode of the isolated structure for small seismic events, for a wide range of frequency content, despite its being very much stiffer when the deflections across the isolators are small (< 5mm).

2. Force-displacement loops and equivalent viscoelastic frequency domain parameters have been used to compare the performance of RBRL systems with different properties.

3. The behaviour characterization of the RBRL device with rubber B has led to the conclusion that it might not be advantageous to use high damping rubber for the tracks.

4. The small-deflection behaviour of the system is highly influenced by the viscoelastic properties of the rubber and hence by the dwell time of the static load. The dependence of $K^{/}$ and μ_{max} on the dwell time appears to be fairly linear with the logarithm of the dwell time.

5. The test results confirmed that the good performance of the RBRL system remains little changed 15 years after the moulding of the rubber tracks.

6. The RBRL system keeps its good performance at small deflections (due to pits effect) also after a large number of sinusoidal vibration at relatively high frequency.

REFERENCES

Ahmadi HR and Muhr AH (1997) Modelling dynamic properties of filled rubber, *Journal of Plastics, Rubber and Composites Processing and Applications*, 26(10): 451-461

Donà M (2015) R*olling-Ball Rubber-Layer system for the lightweight structures seismic protection: experimentation and numerical analyses*, Ph.D. Thesis, University of Trento – Dept. of Civil, Environmental and Mechanical Engineering , Italy (to be published).

Donà M, Muhr AH, Tecchio G, Dusi A, Modena C (2014) *Isolation of light structures with Rolling-Ball Rubber-Layer System - characteristics and performance*, Proceedings of the Second European Conference on Earthquake Engineering and Seismology, Istanbul, Turkey, 25-29 August, paper 1220.

Guerreiro L, Azevedo J, Muhr AH (2007) Seismic Tests and Numerical Modeling of a Rolling-ball Isolation System, *Journal of Earthquake Engineering*, 11(1) :49-66

Muhr AH and Bergamo G (2010) *Shaking Table Tests On Rolling-Ball Rubber-Layer Isolation System*, Proceeding of 14th ECEE 2010, Ohrid, Macedonian, 30 August – 03 September, paper 745